Imaging and Focusing of Atoms by a Fresnel Zone Plate

O. Carnal, M. Sigel, T. Sleator, H. Takuma,[a] and J. Mlynek
Fakultät für Physik, Universität Konstanz, D-7750 Konstanz, Germany
(Received 26 August 1991)

Focusing of and imaging with atoms by means of a spherical Fresnel zone plate has been observed for the first time. An intense beam of metastable helium atoms with atomic de Broglie wavelength $\lambda_{dB}=0.5$–2.5 Å is passed through either a single or a double slit with dimensions in the 10-μm range. This transverse intensity distribution is imaged by a Fresnel zone plate, 210 μm in diameter and with an innermost zone diameter of 18.76 μm. For $\lambda_{dB}=1.96$ Å the focal length is 0.45 m. The imaging properties of the zone plate are presented and compared with numerical calculations.

PACS numbers: 42.80.Bi, 35.80.+s

In analogy to classical optics, the field of *atom optics* deals with the realization of optical elements, such as lenses, mirrors, and beam splitters for atoms. Since atoms, unlike electrons, carry no charge and, unlike neutrons, do not penetrate through matter, new techniques have to be developed to provide optics for atoms. In this Letter we report on novel experiments in which atoms are *focused* by a *freestanding microfabricated Fresnel zone plate*. Making lenses for atoms available is of great importance, e.g., for building a microprobe with atomic matter waves to investigate surfaces. Such a microprobe has the potential of achieving high spatial resolution down to the nanometer range with minimal damage to the investigated surfaces due to the very low atom energies of less than 10 meV.

Although zone plates have already been recognized as focusing elements in 1871 [1], they have found only little application in classical optics. In recent years, however, microfabricated Fresnel zone plates have been applied in x-ray microscopy [2] and in the focusing of slow neutron beams [3].

So far, focusing of atoms has been obtained in transmission by static fields (hexapole magnets, quadrupole electrostatic lenses) or light fields [4] and through specular reflection from a curved liquid-helium mirror [5]. Recently, freestanding microfabricated structures have successfully been used for the diffraction of atoms and also applied in the first atom interferometers [6,7]. These results have led us to consider microstructures not only as beam splitters, but also as focusing devices for atoms. Microfabricated zone plates represent stand-alone systems and are therefore easy to handle. In addition, the use of microstructures greatly facilitates the change from one atomic species to another.

Before we present details of our experiment, let us briefly summarize the principle of a Fresnel zone plate, which is described in many textbooks on optics [8]. Since the zone plate consists of alternating transmitting and opaque concentric rings with diameters increasing like the square root of the order of the ring, the transmission function t can be described by

$$t(\rho)=\begin{cases}0, & \text{for } r_{2n}\le\rho<r_{2n+1} \text{ (absorbing zone)},\\ 1, & \text{for } r_{2n+1}\le\rho<r_{2n+2} \text{ (transmitting zone)},\end{cases} \quad (1)$$

with $r_n=\sqrt{n}\,r_1$ ($n=0,1,\ldots,n_{\max}-1$, the number of zones being $2n_{\max}$), r_1 the innermost zone radius, and ρ the distance from the center of the zone plate. A Fresnel zone plate therefore acts as a lens which images an object at a distance A onto images at distances B'_m, where A and B'_m obey the lens equation

$$\frac{1}{A}+\frac{1}{B'_m}=\frac{1}{f_m}=\frac{m\lambda_{dB}}{(r_1)^2}. \quad (2)$$

Here m is any integer, denoting the order of diffraction. The flux into the various orders m is given by

$$\phi_m=\frac{1}{4}\left[\frac{\sin(m\pi/2)}{m\pi/2}\right]^2\phi_i, \quad (3)$$

with ϕ_i the incoming flux. Since the zone plate has a finite aperture, the image of a point source is limited to a minimum size given approximately by [9]

$$D_m=\frac{1}{2(2n_{\max})^{1/2}}\frac{r_1}{m}. \quad (4)$$

In our experiments we used a commercial zone plate [10] with the following dimensions: $r_1=9.38$ μm, $2n_{\max}=128$, and a total diameter of about 210 μm. The thickness of this gold structure is approximately 0.5 μm.

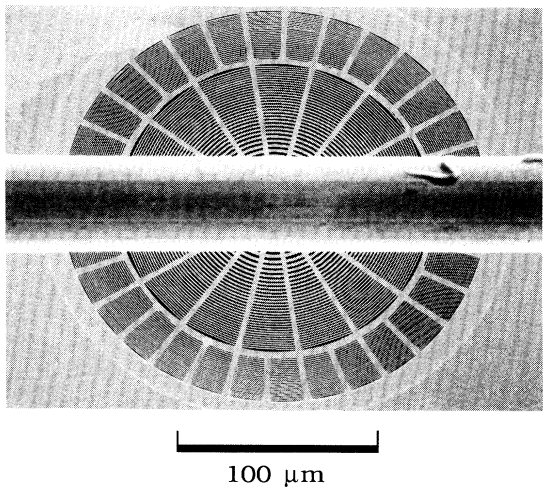

FIG. 1. A scanning electron microscope picture of the zone plate. The wire, 50 μm in diameter, blocks out the zeroth order to increase the contrast in the center of the image plane.

A scanning electron microscope picture of the microfabricated structure is shown in Fig. 1; the use of the wire in front of the zone plate will be discussed later. A thicker support structure is superimposed onto the rings to hold the freestanding microstructure. These radially oriented bars do not have significant influence on the imaging properties of the lens, but reduce the total flux of atoms through the lens by approximately 10%. The resolution of this zone plate is 0.4 μm for the primary focus $m=1$, as given by Eq. (4).

A scheme of our experimental setup is shown in Fig. 2; details of the atomic beam machine are given elsewhere [11]. An intense atomic beam of helium atoms is produced by a supersonic gas expansion through a 25-μm-diam nozzle. The ground-state atoms are then excited into the two metastable states 2^1S_0 and 2^3S_1 by collinear electron impact. After the excitation region, the beam of metastable atoms has a velocity ratio of $v_0/\Delta v \cong 12$–25, depending on the temperature T of the gas reservoir; v_0 denotes the mean velocity in the beam and Δv the full width at half maximum (FWHM) of the Gaussian velocity distribution. By cooling the gas reservoir by a variable flow of liquid helium, T could be set to an arbitrary value between 12 and 300 K. The mean velocity of the atoms could therefore be varied between 380 and 1800 m/sec, corresponding to a $\lambda_{dB}=h/mv_0$ of 0.55 Å up to 2.6 Å. In detailed studies of our beam parameters we observed the following temperature dependence of v_0 and the beam intensity I in the full temperature range:

$$v_0(T) \cong (102\ \text{m/sec})(\sqrt{T[\text{K}]})+60\ \text{m/sec}, \quad (5)$$

$$I(T) \cong (10^{11}\ \text{He}^*/\text{sec sr})(T[\text{K}])^{1.25}. \quad (6)$$

At room temperature the intensity of the beam was around 10^{14} (metastable atoms) $\text{sec}^{-1}\text{sr}^{-1}$, the area of the source of the metastable atoms being approximately 1 mm^2. A decrease in velocity and correspondingly an increase in λ_{dB} is therefore always accompanied by a considerable decrease in the atomic intensity. The pressure in the main experimental chamber was better than 6×10^{-7} mbar. Metastable helium atoms are used since they combine a number of advantages for experiments in atom optics [6].

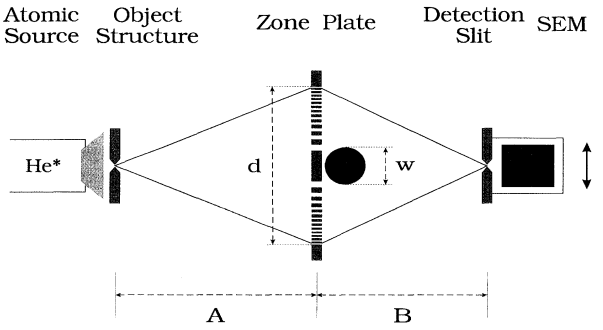

FIG. 2. A schematic of the experimental setup; the dimensions are $A=0.96$ m and $B=0.84$ m, $d=210$ μm, wire diameter $w=50$ μm.

In our focusing experiments the atoms passed through an object structure located a few centimeters behind the electron-impact excitation. As the object, either a single slit or a double slit, both with dimensions in the 10-μm range, were used and imaged by means of the zone plate, located a distance $A=0.96$ m downstream (see Fig. 2). The obtained intensity distributions were then mapped out by transversely scanning a single slit located a distance $B=0.84$ m behind the zone plate; its dimensions were 10 μm in width and 3 mm in height. The total distance $A+B$ was imposed by the dimensions of our beam machine. Mounted on the same translation stage as the detection slit, a secondary electron multiplier (SEM) was used to detect the metastable atoms. The complete detection system could be moved in steps of 3.75 μm by a stepper motor. The pulses generated by the SEM were preamplified, discriminated against background noise, and added up by a counter. The background noise level without atomic beam was around 3 counts/min. We aligned object structure and detection slit parallel to one another to better than 2 mrad using their diffraction pattern from a HeNe laser.

In order for the first-order image distance B_1' to coincide with the distance B between the zone plate and detection plane (for our fixed object distance A) the focal length of the lens had to be tuned to $f_1=0.45$ m by changing λ_{dB} according to Eq. (2). This corresponds to $\lambda_{dB}=1.96$ Å or a nozzle temperature of $T=20$ K. Using only the primary focus for imaging, all other orders, in particular the bright undiffracted zeroth order $m=0$, contribute to an undesired background in the image plane which reduces the image contrast. To block out this background we adjusted a 50-μm-diam metal wire in the center of the zone plate as can be seen in Fig. 2. In two-dimensional imaging this technique is known as "apodizing" which is common practice in x-ray microscopy [2]. At $T=295$ K ($\lambda_{dB}=0.55$ Å), where the various diffrac-

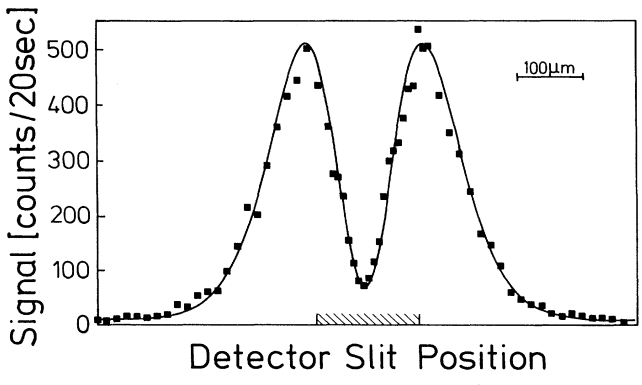

FIG. 3. Atomic intensity distribution in the detector plane at $T=295$ K. The squares represent the experimental values while the solid line is a fitted curve. The shaded region indicates the scan range in Figs. 4 and 5.

tion orders still substantially overlap in the image plane, the "shadow" of the wire was nicely observed in the center of the geometrical image of the zone plate aperture (Fig. 3). This shadow proved helpful in locating the image of the object structures, insofar as after cooling down the gas reservoir the image would appear exactly at the position where the minimum in the shadow had previously been observed. In the following studies scans have been performed only in the shaded region shown in Fig. 3.

In a first experiment a single 10 ± 1-μm slit [see inset of Fig. 4(a)], identical to the detection slit, was used as the object. An intensity distribution obtained in the image plane at $T=20.5$ K is displayed in Fig. 4(a). The transverse scan of the detection slit was done in steps of 3.75 μm with an integration time of 5 min per position. During the scan the temperature was kept constant to within ± 0.5 K. A Gaussian on top of a parabola plus a constant background has been fitted to the experimental data and is displayed as a solid line; thereby, the parabolic part of the signal is attributed to the remaining shadow of the wire [see Fig. 5(a)]. This fit approach can be justified by numerical calculations (see below). The FWHM of this Gaussian was 18 ± 1 μm, the error being the standard deviation of the fitted width; this is only slightly broader than the 16 μm predicted by our numerical calculations. Image peak visibility was better than 70% while more than 95% can be expected from the computation, and the atomic flux in the intensity peak amounted to 17% of the total particle flux through the lens, not far from the predicted 20% [see Eq. (3)]. Because of the absorption of the zone plate and wire this 17% corresponds to only 6% of the atomic flux before the zone plate. The remaining discrepancies could be due to background gas scattering and imperfect alignment of object and detection slits. We also have been able to observe a third-order image of this single slit for $T=200 \pm 15$ K ($\lambda_{dB}=0.66 \pm 0.03$ Å). For this image the prediction from Eq. (2) is $\lambda_{dB}=0.65$ Å; in accordance with Eq. (3) the ratio between flux in the image peak and total transmitted flux was around 1%.

To work out the *imaging* character of the Fresnel zone plate, in a second experiment a self-fabricated double slit was used as the object. Its slit distance was $d_2=49 \pm 2$ μm, the width of the individual slits $s_2=22 \pm 1$ μm, and its height approximately 5 mm [see inset of Fig. 4(b)]. The observed "atomic image" is shown in Fig. 4(b); the two maxima corresponding to the two slits can clearly be identified. The solid line is again a least-squares fit with two Gaussians—the center-to-center distance and width of the two Gaussians being 43 ± 1 and 19 ± 1 μm, respectively. As is clear from the ratio of A and B in our setup we expect an image reduced to $\frac{7}{8}$ of the object size, which is in excellent agreement with the experiment. We have also been able to image an even narrower double slit; under the present experimental conditions, however, the signal-to-noise ratio became rather poor.

In order to study the dependence of the intensity distribution in the detector plane on the atomic wavelength, we investigated the transverse intensity distribution in the detection plane for various nozzle temperatures T in the

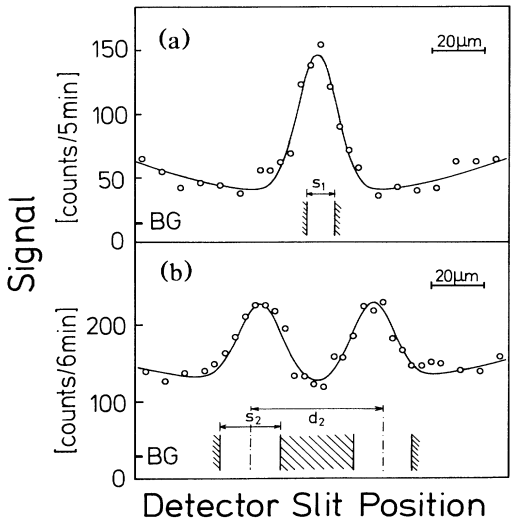

FIG. 4. Image of a single slit (a) and a double slit (b) at $T=20.5$ K. The dots represent the experimental data and the solid line is a fit through the data points. The slit dimensions, as shown in the insets, are $s_1=10$ μm for the single slit and $d_2=49$ μm and $s_2=22$ μm for the double slit. BG denotes the detector background level. The two insets give the dimensions of the corresponding object structures (to scale).

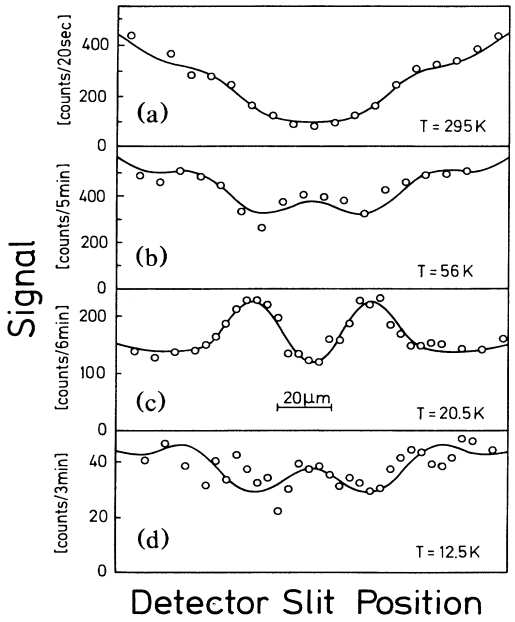

FIG. 5. Image of the double slit at four different nozzle temperatures: (a) $T=295$ K ($\lambda_{dB}=0.55$ Å), (b) $T=56$ K ($\lambda_{dB}=1.2$ Å), (c) $T=20.5$ K ($\lambda_{dB}=1.96$ Å), (d) $T=12.5$ K ($\lambda_{dB}=2.5$ Å). The data are marked by dots and the adjusted numerical calculations by solid lines. For further details see text.

case of the double slit as the object. In addition to the previously discussed double-slit image, Fig. 5 shows scans for $T=12.5$, 56, and 295 K, where the stability of T is better than ± 0.5 K during each scan. An image was only obtained for $T=20.5$ K, whereas more complex patterns appeared at the other temperatures.

To compare the experimental results with theory we have performed numerical simulations of our experiment, integrating the atomic wave amplitude along all paths over the zone plate, including the 50-μm wire, and incoherently summing over all source points. The finite width of the detector slit and the measured velocity distribution have been taken into account. The numerical results were matched to the experimental values by adjusting their position and a scaling factor along the ordinate. As can be seen in Fig. 5, the simulations are in good qualitative agreement with the intensity distributions for the "focusing" wavelength as well as for the structures observed for other wavelengths. The discrepancies for $T=12.5$ K are mainly due to the poor signal-to-noise ratio at this low temperature.

In summary, we point out that the presented lens for atoms exhibits convincing imaging properties and is able to focus around 6% of the incoming particle flux. The disturbing effect of the zeroth order and the related decrease in the image contrast can be drastically reduced by a wire in front of the zone plate or, in two-dimensional imaging, by an apodized zone plate. Modern technologies in electron lithography allow the fabrication of structures smaller than 100 nm in size, which would increase the area of the zone plate by more than a factor of 4. On the other hand, more homoenergetic atomic beams would allow one to reach the theoretical resolution given by Eq. (4). Such atomic beams can be prepared, e.g., by special laser cooling techniques [12]. First experiments to demonstrate the two-dimensional imaging of structures below 1 μm would be further steps towards the realization of an atomic "microprobe."

We thank R. Leonhardt and H. Görig for their help and patience during our first experiments with liquid helium. We are indebted to T. Pfau for manufacturing the double-slit structures and to J. Hentschel for the electron microscope pictures. S. Hahn is acknowledged for his technical assistance. One of us (T.S.) is grateful to the Alexander von Humboldt Foundation for financial support. H.T. acknowledges support from the Deutsche Forschungsgemeinschaft for a guest professorship. This work was supported by the Deutsche Forschungsgemeinschaft.

[a]Permanent address: Institute of Laser Science, University of Electro-Communications, Tokyo 182, Japan.

[1] Lord Rayleigh seems to have invented the zone plate in 1871; the first appearance in literature is J. L. Soret, Ann. Phys. **156**, 99 (1875).

[2] See, e.g., *X-Ray Microscopy,* edited by G. Schmahl and D. Rudolph, Springer Series in Optical Sciences Vol. 43 (Springer, Berlin, 1984).

[3] P. D. Kearney, A. G. Klein, G. I. Opat, and R. Gähler, Nature (London) **287**, 313 (1980).

[4] J. E. Bjorkholm, R. E. Freeman, A. Ashkin, and D. B. Pearson, Phys. Rev. Lett. **41**, 1361 (1978); V. I. Balykin, V. S. Letokhov, A. I. Sidorov, and Yu. B. Ovchinnikov, J. Mod. Opt. **35**, 17 (1988).

[5] J. J. Berkhout, O. J. Luiten, I. D. Setija, T. W. Hijmans, T. Mizusaki, and J. T. M. Walraven, Phys. Rev. Lett. **63**, 1689 (1989).

[6] O. Carnal and J. Mlynek, Phys. Rev. Lett. **66**, 2689 (1991).

[7] D. W. Keith, C. R. Ekstrom, Q. A. Turchette, and D. E. Pritchard, Phys. Rev. Lett. **66**, 2693 (1991).

[8] See, e.g., E. Hecht, *Optics* (Addison-Wesley, Reading, MA, 1989), 2nd ed., p. 445.

[9] J.-A. Sun and A. Cai, J. Opt. Soc. Am. A **8**, 33 (1991).

[10] Heidenhain Inc., Traunreut, Germany.

[11] O. Carnal, Ph.D. thesis, Eidgenössische Technische Hochschule Zürich, 1991 (unpublished).

[12] A. Faulstich *et al.* (to be published); T. Sleator, O. Carnal, A. Faulstich, and J. Mlynek, in "Quantum Measurements in Optics," Proceedings of the NATO Advanced Research Workshop, edited by P. Tombesi and D. Walls (to be published).

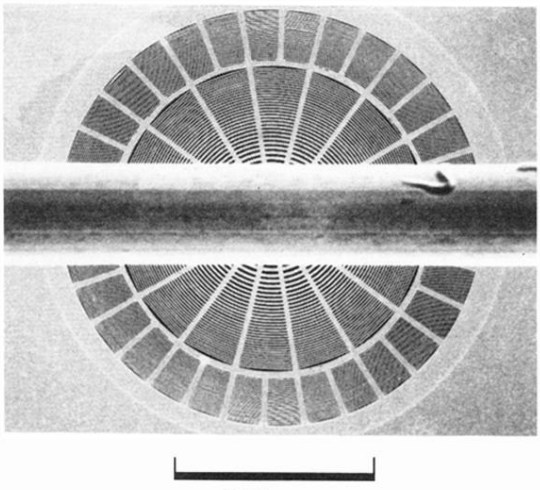

FIG. 1. A scanning electron microscope picture of the zone plate. The wire, 50 μm in diameter, blocks out the zeroth order to increase the contrast in the center of the image plane.